Observation of J/ψ Electromagnetic Dalitz Decays to $X(1835)$, $X(2120)$, and $X(2370)$

M. Ablikim,[1] M. N. Achasov,[10,c] P. Adlarson,[67] S. Ahmed,[15] M. Albrecht,[4] R. Aliberti,[28] A. Amoroso,[66a,66c] M. R. An,[32] Q. An,[63,49] X. H. Bai,[57] Y. Bai,[48] O. Bakina,[29] R. Baldini Ferroli,[23a] I. Balossino,[24a] Y. Ban,[38,k] K. Begzsuren,[26] N. Berger,[28] M. Bertani,[23a] D. Bettoni,[24a] F. Bianchi,[66a,66c] J. Bloms,[60] A. Bortone,[66a,66c] I. Boyko,[29] R. A. Briere,[5] H. Cai,[68] X. Cai,[1,49] A. Calcaterra,[23a] G. F. Cao,[1,54] N. Cao,[1,54] S. A. Cetin,[53a] J. F. Chang,[1,49] W. L. Chang,[1,54] G. Chelkov,[29,b] D. Y. Chen,[6] G. Chen,[1] H. S. Chen,[1,54] M. L. Chen,[1,49] S. J. Chen,[35] X. R. Chen,[25] Y. B. Chen,[1,49] Z. J. Chen,[20,l] W. S. Cheng,[66c] G. Cibinetto,[24a] F. Cossio,[66c] X. F. Cui,[36] H. L. Dai,[1,49] X. C. Dai,[1,54] A. Dbeyssi,[15] R. E. de Boer,[4] D. Dedovich,[29] Z. Y. Deng,[1] A. Denig,[28] I. Denysenko,[29] M. Destefanis,[66a,66c] F. De Mori,[66a,66c] Y. Ding,[33] C. Dong,[36] J. Dong,[1,49] L. Y. Dong,[1,54] M. Y. Dong,[1,49,54] X. Dong,[68] S. X. Du,[71] Y. L. Fan,[68] J. Fang,[1,49] S. S. Fang,[1,54] Y. Fang,[1] R. Farinelli,[24a] L. Fava,[66b,66c] F. Feldbauer,[4] G. Felici,[23a] C. Q. Feng,[63,49] J. H. Feng,[50] M. Fritsch,[4] C. D. Fu,[1] Y. Gao,[63,49] Y. Gao,[38,k] Y. Gao,[64] Y. G. Gao,[6] I. Garzia,[24a,24b] P. T. Ge,[68] C. Geng,[50] E. M. Gersabeck,[58] A. Gilman,[61] K. Goetzen,[11] L. Gong,[33] W. X. Gong,[1,49] W. Gradl,[28] M. Greco,[66a,66c] L. M. Gu,[35] M. H. Gu,[1,49] S. Gu,[2] Y. T. Gu,[13] C. Y. Guan,[1,54] A. Q. Guo,[22] L. B. Guo,[34] R. P. Guo,[40] Y. P. Guo,[9,h] A. Guskov,[29,b] T. T. Han,[41] W. Y. Han,[32] X. Q. Hao,[16] F. A. Harris,[56] K. L. He,[1,54] F. H. Heinsius,[4] C. H. Heinz,[28] T. Held,[4] Y. K. Heng,[1,49,54] C. Herold,[51] M. Himmelreich,[11,f] T. Holtmann,[4] G. Y. Hou,[1,54] Y. R. Hou,[54] Z. L. Hou,[1] H. M. Hu,[1,54] J. F. Hu,[47,m] T. Hu,[1,49,54] Y. Hu,[1] G. S. Huang,[63,49] L. Q. Huang,[64] X. T. Huang,[41] Y. P. Huang,[1] Z. Huang,[38,k] T. Hussain,[65] N. Hüsken,[22,28] W. Ikegami Andersson,[67] W. Imoehl,[22] M. Irshad,[63,49] S. Jaeger,[4] S. Janchiv,[26,j] Q. Ji,[1] Q. P. Ji,[16] X. B. Ji,[1,54] X. L. Ji,[1,49] Y. Y. Ji,[41] H. B. Jiang,[41] X. S. Jiang,[1,49,54] J. B. Jiao,[41] Z. Jiao,[18] S. Jin,[35] Y. Jin,[57] M. Q. Jing,[1,54] T. Johansson,[67] N. Kalantar-Nayestanaki,[55] X. S. Kang,[33] R. Kappert,[55] M. Kavatsyuk,[55] B. C. Ke,[43,1] I. K. Keshk,[4] A. Khoukaz,[60] P. Kiese,[28] R. Kiuchi,[1] R. Kliemt,[11] L. Koch,[30] O. B. Kolcu,[53a,e] B. Kopf,[4] M. Kuemmel,[4] M. Kuessner,[4] A. Kupsc,[67] M. G. Kurth,[1,54] W. Kühn,[30] J. J. Lane,[58] J. S. Lange,[30] P. Larin,[15] A. Lavania,[21] L. Lavezzi,[66a,66c] Z. H. Lei,[63,49] H. Leithoff,[28] M. Lellmann,[28] T. Lenz,[28] C. Li,[39] C. H. Li,[32] Cheng Li,[63,49] D. M. Li,[71] F. Li,[1,49] G. Li,[1] H. Li,[63,49] H. Li,[43] H. B. Li,[1,54] H. J. Li,[16] J. L. Li,[41] J. Q. Li,[4] J. S. Li,[50] Ke Li,[1] L. K. Li,[1] Lei Li,[3] P. R. Li,[31,n,o] S. Y. Li,[52] W. D. Li,[1,54] W. G. Li,[1] X. H. Li,[63,49] X. L. Li,[41] Xiaoyu Li,[1,54] Z. Y. Li,[50] H. Liang,[1,54] H. Liang,[63,49] H. Liang,[27] Y. F. Liang,[45] Y. T. Liang,[25] G. R. Liao,[12] L. Z. Liao,[1,54] J. Libby,[21] C. X. Lin,[50] B. J. Liu,[1] C. X. Liu,[1] D. Liu,[15,63] F. H. Liu,[44] Fang Liu,[1] Feng Liu,[6] H. B. Liu,[13] H. M. Liu,[1,54] Huanhuan Liu,[1] Huihui Liu,[17] J. B. Liu,[63,49] J. L. Liu,[64] J. Y. Liu,[1,54] K. Liu,[1] K. Y. Liu,[33] L. Liu,[63,49] M. H. Liu,[9,h] P. L. Liu,[1] Q. Liu,[68] Q. Liu,[54] S. B. Liu,[63,49] Shuai Liu,[46] T. Liu,[1,54] W. M. Liu,[63,49] X. Liu,[31,n,o] Y. Liu,[31,n,o] Y. B. Liu,[36] Z. A. Liu,[1,49,54] Z. Q. Liu,[41] X. C. Lou,[1,49,54] F. X. Lu,[50] H. J. Lu,[18] J. D. Lu,[1,54] J. G. Lu,[1,49] X. L. Lu,[1] Y. Lu,[1] Y. P. Lu,[1,49] C. L. Luo,[34] M. X. Luo,[70] P. W. Luo,[50] T. Luo,[9,h] X. L. Luo,[1,49] X. R. Lyu,[54] F. C. Ma,[33] H. L. Ma,[1] L. L. Ma,[41] M. M. Ma,[1,54] Q. M. Ma,[1] R. Q. Ma,[1,54] R. T. Ma,[54] X. X. Ma,[1,54] X. Y. Ma,[1,49] F. E. Maas,[15] M. Maggiora,[66a,66c] S. Maldaner,[4] S. Malde,[61] Q. A. Malik,[65] A. Mangoni,[23b] Y. J. Mao,[38,k] Z. P. Mao,[1] S. Marcello,[66a,66c] Z. X. Meng,[57] J. G. Messchendorp,[55] G. Mezzadri,[24a] T. J. Min,[35] R. E. Mitchell,[22] X. H. Mo,[1,49,54] Y. J. Mo,[6] N. Yu. Muchnoi,[10,c] H. Muramatsu,[59] S. Nakhoul,[11,f] Y. Nefedov,[29] F. Nerling,[11,f] I. B. Nikolaev,[10,c] Z. Ning,[1,49] S. Nisar,[8,i] S. L. Olsen,[54] Q. Ouyang,[1,49,54] S. Pacetti,[23b,23c] X. Pan,[9,h] Y. Pan,[58] A. Pathak,[1] P. Patteri,[23a] M. Pelizaeus,[4] H. P. Peng,[63,49] K. Peters,[11,f] J. Pettersson,[67] J. L. Ping,[34] R. G. Ping,[1,54] R. Poling,[59] V. Prasad,[63,49] H. Qi,[63,49] H. R. Qi,[52] K. H. Qi,[25] M. Qi,[35] T. Y. Qi,[9] S. Qian,[1,49] W. B. Qian,[54] Z. Qian,[50] C. F. Qiao,[54] L. Q. Qin,[12] X. P. Qin,[9] X. S. Qin,[41] Z. H. Qin,[1,49] J. F. Qiu,[1] S. Q. Qu,[36] K. H. Rashid,[65] K. Ravindran,[21] C. F. Redmer,[28] A. Rivetti,[66c] V. Rodin,[55] M. Rolo,[66c] G. Rong,[1,54] Ch. Rosner,[15] M. Rump,[60] H. S. Sang,[63] A. Sarantsev,[29,d] Y. Schelhaas,[28] C. Schnier,[4] K. Schoenning,[67] M. Scodeggio,[24a,24b] D. C. Shan,[46] W. Shan,[19] X. Y. Shan,[63,49] J. F. Shangguan,[46] M. Shao,[63,49] C. P. Shen,[9] H. F. Shen,[1,54] P. X. Shen,[36] X. Y. Shen,[1,54] H. C. Shi,[63,49] R. S. Shi,[1,54] X. Shi,[1,49] X. D. Shi,[63,49] J. J. Song,[41] W. M. Song,[27,1] Y. X. Song,[38,k] S. Sosio,[66a,66c] S. Spataro,[66a,66c] K. X. Su,[68] P. P. Su,[46] F. F. Sui,[41] G. X. Sun,[1] H. K. Sun,[1] J. F. Sun,[16] L. Sun,[68] S. S. Sun,[1,54] T. Sun,[1,54] W. Y. Sun,[34] W. Y. Sun,[27] X. Sun,[20,l] Y. J. Sun,[63,49] Y. K. Sun,[63,49] Y. Z. Sun,[1] Z. T. Sun,[1] Y. H. Tan,[68] Y. X. Tan,[63,49] C. J. Tang,[45] G. Y. Tang,[1] J. Tang,[50] J. X. Teng,[63,49] V. Thoren,[67] W. H. Tian,[43] Y. T. Tian,[25] I. Uman,[53b] B. Wang,[1] C. W. Wang,[35] D. Y. Wang,[38,k] H. J. Wang,[31,n,o] H. P. Wang,[1,54] K. Wang,[1,49] L. L. Wang,[1] M. Wang,[41] M. Z. Wang,[38,k] Meng Wang,[1,54] W. Wang,[50] W. H. Wang,[68] W. P. Wang,[63,49] X. Wang,[38,k] X. F. Wang,[31,n,o] X. L. Wang,[9,h] Y. Wang,[50] Y. Wang,[63,49] Y. D. Wang,[37] Y. F. Wang,[1,49,54] Y. Q. Wang,[1] Y. Y. Wang,[31,n,o] Z. Wang,[1,49] Z. Y. Wang,[1] Ziyi Wang,[54] Zongyuan Wang,[1,54] D. H. Wei,[12] F. Weidner,[60] S. P. Wen,[1] D. J. White,[58] U. Wiedner,[4] G. Wilkinson,[61] M. Wolke,[67] L. Wollenberg,[4] J. F. Wu,[1,54] L. H. Wu,[1] L. J. Wu,[1,54] X. Wu,[9,h] Z. Wu,[1,49] L. Xia,[63,49] H. Xiao,[9,h] S. Y. Xiao,[1] Z. J. Xiao,[34] X. H. Xie,[38,k] Y. G. Xie,[1,49] Y. H. Xie,[6] T. Y. Xing,[1,54] G. F. Xu,[1] Q. J. Xu,[14] W. Xu,[1,54] X. P. Xu,[46] Y. C. Xu,[54] F. Yan,[9,h] L. Yan,[9,h] W. B. Yan,[63,49] W. C. Yan,[71] Xu Yan,[46] H. J. Yang,[42,g] H. X. Yang,[1]

L. Yang,[43] S. L. Yang,[54] Y. X. Yang,[12] Yifan Yang,[1,54] Zhi Yang,[25] M. Ye,[1,49] M. H. Ye,[7] J. H. Yin,[1] Z. Y. You,[50] B. X. Yu,[1,49,54] C. X. Yu,[36] G. Yu,[1,54] J. S. Yu,[20,l] T. Yu,[64] C. Z. Yuan,[1,54] L. Yuan,[2] X. Q. Yuan,[38,k] Y. Yuan,[1] Z. Y. Yuan,[50] C. X. Yue,[32] A. Yuncu,[53a,a] A. A. Zafar,[65] X. Zeng,[6] Y. Zeng,[20,l] A. Q. Zhang,[1] B. X. Zhang,[1] Guangyi Zhang,[16] H. Zhang,[63] H. H. Zhang,[50] H. H. Zhang,[27] H. Y. Zhang,[1,49] J. J. Zhang,[43] J. L. Zhang,[69] J. Q. Zhang,[34] J. W. Zhang,[1,49,54] J. Y. Zhang,[1] J. Z. Zhang,[1,54] Jianyu Zhang,[1,54] Jiawei Zhang,[1,54] L. M. Zhang,[52] L. Q. Zhang,[50] Lei Zhang,[35] S. Zhang,[50] S. F. Zhang,[35] Shulei Zhang,[20,l] X. D. Zhang,[37] X. Y. Zhang,[41] Y. Zhang,[61] Y. H. Zhang,[1,49] Y. T. Zhang,[63,49] Yan Zhang,[63,49] Yao Zhang,[1] Yi Zhang,[9,h] Z. H. Zhang,[6] Z. Y. Zhang,[68] G. Zhao,[1] J. Zhao,[32] J. Y. Zhao,[1,54] J. Z. Zhao,[1,49] Lei Zhao,[63,49] Ling Zhao,[1] M. G. Zhao,[36] Q. Zhao,[1] S. J. Zhao,[71] Y. B. Zhao,[1,49] Y. X. Zhao,[25] Z. G. Zhao,[63,49] A. Zhemchugov,[29,b] B. Zheng,[64] J. P. Zheng,[1,49] Y. Zheng,[38,k] Y. H. Zheng,[54] B. Zhong,[34] C. Zhong,[64] L. P. Zhou,[1,54] Q. Zhou,[1,54] X. Zhou,[68] X. K. Zhou,[54] X. R. Zhou,[63,49] X. Y. Zhou,[32] A. N. Zhu,[1,54] J. Zhu,[36] K. Zhu,[1] K. J. Zhu,[1,49,54] S. H. Zhu,[62] T. J. Zhu,[69] W. J. Zhu,[9,h] W. J. Zhu,[36] Y. C. Zhu,[63,49] Z. A. Zhu,[1,54] B. S. Zou,[1] and J. H. Zou[1]

(BESIII Collaboration)

[1]*Institute of High Energy Physics, Beijing 100049, People's Republic of China*
[2]*Beihang University, Beijing 100191, People's Republic of China*
[3]*Beijing Institute of Petrochemical Technology, Beijing 102617, People's Republic of China*
[4]*Bochum Ruhr-University, D-44780 Bochum, Germany*
[5]*Carnegie Mellon University, Pittsburgh, Pennsylvania 15213, USA*
[6]*Central China Normal University, Wuhan 430079, People's Republic of China*
[7]*China Center of Advanced Science and Technology, Beijing 100190, People's Republic of China*
[8]*COMSATS University Islamabad, Lahore Campus, Defence Road, Off Raiwind Road, 54000 Lahore, Pakistan*
[9]*Fudan University, Shanghai 200443, People's Republic of China*
[10]*G.I. Budker Institute of Nuclear Physics SB RAS (BINP), Novosibirsk 630090, Russia*
[11]*GSI Helmholtzcentre for Heavy Ion Research GmbH, D-64291 Darmstadt, Germany*
[12]*Guangxi Normal University, Guilin 541004, People's Republic of China*
[13]*Guangxi University, Nanning 530004, People's Republic of China*
[14]*Hangzhou Normal University, Hangzhou 310036, People's Republic of China*
[15]*Helmholtz Institute Mainz, Staudinger Weg 18, D-55099 Mainz, Germany*
[16]*Henan Normal University, Xinxiang 453007, People's Republic of China*
[17]*Henan University of Science and Technology, Luoyang 471003, People's Republic of China*
[18]*Huangshan College, Huangshan 245000, People's Republic of China*
[19]*Hunan Normal University, Changsha 410081, People's Republic of China*
[20]*Hunan University, Changsha 410082, People's Republic of China*
[21]*Indian Institute of Technology Madras, Chennai 600036, India*
[22]*Indiana University, Bloomington, Indiana 47405, USA*
[23a]*INFN Laboratori Nazionali di Frascati, (A)INFN Laboratori Nazionali di Frascati, I-00044 Frascati, Italy*
[23b]*INFN Laboratori Nazionali di Frascati, INFN Sezione di Perugia, I-06100 Perugia, Italy*
[23c]*INFN Laboratori Nazionali di Frascati, University of Perugia, I-06100 Perugia, Italy*
[24a]*INFN Sezione di Ferrara, INFN Sezione di Ferrara, I-44122 Ferrara, Italy*
[24b]*INFN Sezione di Ferrara, University of Ferrara, I-44122 Ferrara, Italy*
[25]*Institute of Modern Physics, Lanzhou 730000, People's Republic of China*
[26]*Institute of Physics and Technology, Peace Avenue 54B, Ulaanbaatar 13330, Mongolia*
[27]*Jilin University, Changchun 130012, People's Republic of China*
[28]*Johannes Gutenberg University of Mainz, Johann-Joachim-Becher-Weg 45, D-55099 Mainz, Germany*
[29]*Joint Institute for Nuclear Research, 141980 Dubna, Moscow region, Russia*
[30]*Justus-Liebig-Universitaet Giessen, II. Physikalisches Institut, Heinrich-Buff-Ring 16, D-35392 Giessen, Germany*
[31]*Lanzhou University, Lanzhou 730000, People's Republic of China*
[32]*Liaoning Normal University, Dalian 116029, People's Republic of China*
[33]*Liaoning University, Shenyang 110036, People's Republic of China*
[34]*Nanjing Normal University, Nanjing 210023, People's Republic of China*
[35]*Nanjing University, Nanjing 210093, People's Republic of China*
[36]*Nankai University, Tianjin 300071, People's Republic of China*
[37]*North China Electric Power University, Beijing 102206, People's Republic of China*
[38]*Peking University, Beijing 100871, People's Republic of China*
[39]*Qufu Normal University, Qufu 273165, People's Republic of China*
[40]*Shandong Normal University, Jinan 250014, People's Republic of China*
[41]*Shandong University, Jinan 250100, People's Republic of China*

[42]Shanghai Jiao Tong University, Shanghai 200240, People's Republic of China
[43]Shanxi Normal University, Linfen 041004, People's Republic of China
[44]Shanxi University, Taiyuan 030006, People's Republic of China
[45]Sichuan University, Chengdu 610064, People's Republic of China
[46]Soochow University, Suzhou 215006, People's Republic of China
[47]South China Normal University, Guangzhou 510006, People's Republic of China
[48]Southeast University, Nanjing 211100, People's Republic of China
[49]State Key Laboratory of Particle Detection and Electronics, Beijing 100049, Hefei 230026, People's Republic of China
[50]Sun Yat-Sen University, Guangzhou 510275, People's Republic of China
[51]Suranaree University of Technology, University Avenue 111, Nakhon Ratchasima 30000, Thailand
[52]Tsinghua University, Beijing 100084, People's Republic of China
[53a]Turkish Accelerator Center Particle Factory Group, Istanbul Bilgi University, 34060 Eyup, Istanbul, Turkey
[53b]Turkish Accelerator Center Particle Factory Group, Near East University, 99138 Nicosia, North Cyprus, Mersin 10, Turkey
[54]University of Chinese Academy of Sciences, Beijing 100049, People's Republic of China
[55]University of Groningen, NL-9747 AA Groningen, The Netherlands
[56]University of Hawaii, Honolulu, Hawaii 96822, USA
[57]University of Jinan, Jinan 250022, People's Republic of China
[58]University of Manchester, Oxford Road, Manchester M13 9PL, United Kingdom
[59]University of Minnesota, Minneapolis, Minnesota 55455, USA
[60]University of Muenster, Wilhelm-Klemm-Strasse 9, 48149 Muenster, Germany
[61]University of Oxford, Keble Road, Oxford, United Kingdom, OX13RH
[62]University of Science and Technology Liaoning, Anshan 114051, People's Republic of China
[63]University of Science and Technology of China, Hefei 230026, People's Republic of China
[64]University of South China, Hengyang 421001, People's Republic of China
[65]University of the Punjab, Lahore-54590, Pakistan
[66a]University of Turin and INFN, University of Turin, I-10125 Turin, Italy
[66b]University of Turin and INFN, University of Eastern Piedmont, I-15121 Alessandria, Italy
[66c]University of Turin and INFN, INFN, I-10125 Turin, Italy
[67]Uppsala University, Box 516, SE-75120 Uppsala, Sweden
[68]Wuhan University, Wuhan 430072, People's Republic of China
[69]Xinyang Normal University, Xinyang 464000, People's Republic of China
[70]Zhejiang University, Hangzhou 310027, People's Republic of China
[71]Zhengzhou University, Zhengzhou 450001, People's Republic of China

(Received 30 December 2021; revised 7 April 2022; accepted 8 June 2022; published 6 July 2022)

Using a sample of about 10^{10} J/ψ events collected at a center-of-mass energy $\sqrt{s} = 3.097$ GeV with the BESIII detector, the electromagnetic Dalitz decays $J/\psi \to e^+e^-\pi^+\pi^-\eta'$, with $\eta' \to \gamma\pi^+\pi^-$ and $\eta' \to \pi^+\pi^-\eta$, have been studied. The decay $J/\psi \to e^+e^-X(1835)$ is observed with a significance of 15σ, and also an e^+e^- invariant-mass dependent transition form factor of $J/\psi \to e^+e^-X(1835)$ is presented for the first time. The intermediate states $X(2120)$ and $X(2370)$ are also observed in the $\pi^+\pi^-\eta'$ invariant-mass spectrum with significances of 5.3σ and 7.3σ. The corresponding product branching fractions for $J/\psi \to e^+e^-X$, $X \to \pi^+\pi^-\eta'$ [$X = X(1835)$, $X(2120)$, and $X(2370)$] are reported.

DOI: 10.1103/PhysRevLett.129.022002

The state $X(1835)$ was first discovered by the BESII experiment in $J/\psi \to \gamma\pi^+\pi^-\eta'$ decays [1] in 2005. In 2011, the discovery was confirmed by the BESIII experiment [2] in the same channel. Later, using an order of magnitude larger data sample, BESIII performed a study of the $\pi^+\pi^-\eta'$ line shape of the $X(1835)$ and reported a significant abrupt change in the slope of the $\pi^+\pi^-\eta'$ invariant-mass distribution at the proton-antiproton ($p\bar{p}$) mass threshold [3]. The study supported the existence of a $p\bar{p}$ moleculelike or bound state but no further conclusion was drawn with the limited statistic at that moment. Further study indicates that the $X(1835)$ shares the same spin parity 0^{-+} [4,5] with the $X(p\bar{p})$, a $p\bar{p}$ bound state, which has been observed by the BES [6] and confirmed by BESIII [7] and CLEO [8]. Many theoretical speculations believe that the $X(1835)$ is exactly a kind of $p\bar{p}$ bound state [9–11]; however, the $X(1835)$ has not been observed in other processes, such as

$\Upsilon(1S) \to \gamma p\bar{p}$ [12], $J/\psi \to \omega p\bar{p}$ [13], and $J/\psi \to \phi p\bar{p}$ [14]. The nature of the $X(1835)$ is still controversial.

Furthermore, BESIII observed three other resonance states—the $X(2120)$ [2], $X(2370)$ [2], and $X(2600)$ [15] —in $J/\psi \to \gamma\pi^+\pi^-\eta'$ decays. The unprecedented sample of about 10^{10} J/ψ decays collected with the BESIII detector allows confirmation of the $X(1835)$, $X(2120)$, $X(2370)$, and $X(2600)$ states in different J/ψ decay modes, in particular, $J/\psi \to e^+e^-\pi^+\pi^-\eta'$.

These electromagnetic (EM) Dalitz decays, where an off-shell photon is internally converted into an e^+e^- pair, provide an ideal opportunity to probe the structure of hadronic states and to investigate the fundamental mechanisms of the interactions between photons and hadrons [16]. Such EM decays are found to be simpler and they allow one to make a more complete theoretical interpretation than the case for pure hadronic interactions. Consequently, these EM Dalitz decays constitute a testing ground for any theory describing the structure of strongly interacting particles [16].

In theory, for the EM Dalitz decay $J/\psi \to e^+e^-X(1835)$, assuming pointlike particles, the branching fraction of the Dalitz decay can be exactly described by quantum electrodynamics (QED) in the standard model [16], and the theoretical branching ratio, $R \equiv \{\mathcal{B}[J/\psi \to e^+e^-X(1835)]/\mathcal{B}[J/\psi \to \gamma X(1835)]\}$, is calculated to be 9.80×10^{-3} [17], where many theoretical uncertainties cancel. The first measurement of the branching fraction of the EM Dalitz decay and the ratio R will provide a straightforward test of this pointlike QED prediction.

The EM Dalitz decay $J/\psi \to e^+e^-X(1835)$ gives access to the EM transition form factors (TFFs) between the J/ψ and $X(1835)$ states. The q^2-dependent differential decay rate of $J/\psi \to e^+e^-X(1835)$ normalized to the corresponding radiative decay $J/\psi \to \gamma X(1835)$ can be expressed as [16,18,19]

$$\frac{d\Gamma(J/\psi \to X(1835)e^+e^-)}{dq^2\Gamma(J/\psi \to X(1835)\gamma)} = |F(q^2)|^2 \times [\mathrm{QED}(q^2)], \quad (1)$$

where the normalized TFF for the $J/\psi \to X(1835)$ transition is defined as $|F(q^2)|^2$, q^2 is the square of the invariant mass of the e^+e^- pair, and $[\mathrm{QED}(q^2)]$ [18] represents the QED ratio calculated for pointlike particles. Experimentally, the TFF is directly accessible by comparing the measured invariant-mass spectrum of the lepton pairs from the Dalitz decays with the pointlike QED prediction. The q^2-dependent TFF, which reflects the deviation from the pointlike particle assumption [20], can provide additional information on the interactions between J/ψ and $X(1835)$, and serves as a sensitive probe into their internal structure. Furthermore, it can possibly help in distinguishing the transition mechanisms based on the $q\bar{q}$ scenario and other solutions that alter the simple quark model picture. To be specific, besides the $p\bar{p}$ bound state, there are many different theoretical models for the nature of the $X(1835)$, such as a pseudoscalar glueball [21–23], an excited η' state [24], an excited ϕ state [25], etc. It could be most likely a mixing state of $p\bar{p}$ and $s\bar{s}$ and this idea has been investigated in, e.g., Ref. [26]. Different theoretical models result in different TFFs. Our measurement of the q^2-dependent TFF will be helpful for the theorists when they proceed to predictions based on different assumptions of the $X(1835)$ structure.

In this Letter, we report the observation of the EM Dalitz decays $J/\psi \to e^+e^-X$, where X represents the $X(1835)$, $X(2120)$, and $X(2370)$, and the measurement of TFF for the $J/\psi \to e^+e^-X(1835)$ transition.

This Letter is performed with a sample of $(1.0087 \pm 0.0044) \times 10^{10}$ J/ψ events collected at the center-of-mass energy 3.097 GeV with the BESIII detector operating at the BEPCII [27]. The total number of J/ψ events collected in the years of 2009, 2012, 2018, and 2019 is determined using inclusive J/ψ decays with the method described in Ref. [28]. The BESIII detector is composed of a helium-based main drift chamber (MDC), a time-of-flight system, a CsI(Tl) electromagnetic calorimeter (EMC), and a muon counter. Details about the design and performance of the BESIII detector are given in Refs. [29,30]. Monte Carlo (MC) simulated data samples are produced with a GEANT4-based [31] software package, which includes the geometric description of the BESIII detector and the detector response. An inclusive MC sample containing about 10^{10} J/ψ events that includes both the production of the J/ψ meson and the continuum processes incorporated in the event generator KKMC [32] is used to study possible physics backgrounds. The known decay modes of the J/ψ meson are modeled with the event generator EVTGEN [33] using branching fractions taken from the Particle Data Group [34], and the remaining unknown charmonium decays are modeled with the event generator LUNDCHARM [35,36]. Final state radiation from charged final state particles is incorporated using the PHOTOS package [37]. For the simulation of the signal processes, the three $J/\psi \to e^+e^-X$ decay modes are generated with angular distributions according to the amplitude squared in Eq. (3) of Ref. [19] taking into account the J/ψ polarization effect. The final state η' candidates from $X \to \pi^+\pi^-\eta'$ are reconstructed with two decay modes: $\eta' \to \gamma\pi^+\pi^-$ and $\eta' \to \pi^+\pi^-\eta, \eta \to \gamma\gamma$.

Charged tracks are reconstructed in the MDC with a polar-angle (θ) range of $|\cos\theta| < 0.93$. The distance of closest approach of each track to the interaction point must be less than 10 cm along the z axis, and less than 1 cm in the transverse plane. The number of charged tracks is required to be six, with a net charge equal to zero, and exactly two tracks are identified as the electron-positron pair in the final state. Particle identification for charged tracks combines measurements of the energy deposited in the MDC (dE/dx), the flight time in the time-of-flight system, and the EMC information to form probabilities $\mathrm{Prob}(i)_{i=e;\pi;K}$. A track is considered an electron when $\mathrm{Prob}(e)$ is larger than $\mathrm{Prob}(\pi)$ and $\mathrm{Prob}(K)$, and the remaining candidates are identified as pions. Photon candidates are required to have a minimum energy of 25 MeV in the EMC barrel region ($|\cos\theta| < 0.80$) or 50 MeV in the end-cap region ($0.86 < |\cos\theta| < 0.92$), and to be separated from charged tracks by more than 10°.

For the $\eta' \to \gamma\pi^+\pi^-$ decay mode, a four-constraint (4C) kinematic fit imposing conservation of the initial energy and momentum is performed to the hypothesis of $e^+e^-\pi^+\pi^-\pi^+\pi^-\gamma$. For the events with more than one photon candidate, the combination with the minimum χ^2_{4C} is selected, and events with $\chi^2_{4C} < 60$ are retained. The χ^2 selection requirement is optimized for maximal signal (S) to background (B) ratio, i.e., $S/\sqrt{S+B}$. In addition, events with $M_{\gamma e^+e^-} < 210\ \mathrm{MeV}/c^2$, $490 < M_{\gamma e^+e^-} < 600\ \mathrm{MeV}/c^2$, and $700 < M_{\gamma e^+e^-} < 820\ \mathrm{MeV}/c^2$ are removed to suppress background events from $J/\psi \to \pi^0\pi^+\pi^-\pi^+\pi^-$, $J/\psi \to \eta\pi^+\pi^-\pi^+\pi^-$, and $J/\psi \to \omega\pi^+\pi^-\pi^+\pi^-$ (π^0, $\eta \to \gamma e^+e^-$, $\omega \to \pi^0\gamma$, $\pi^0 e^+e^-$), respectively. Here, all mass windows correspond to about 3 times the invariant-mass resolution. Since the $\pi^+\pi^-$ pairs from $\eta' \to \gamma\pi^+\pi^-$ are dominantly from the ρ^0 resonance, their invariant mass must be in the range $575 < M_{\pi^+\pi^-} < 920\ \mathrm{MeV}/c^2$. As shown in Fig. 1(a), η' candidates are selected with $|M_{\gamma\pi^+\pi^-} - m_{\eta'}| < 15\ \mathrm{MeV}/c^2$. Events with $|M_{e^+e^-} - m_\omega| < 25\,\mathrm{MeV}/c^2$ and $|M_{e^+e^-} - m_\phi| < 30\,\mathrm{MeV}/c^2$ are removed to suppress background events from $J/\psi \to \omega\pi^+\pi^-\eta'(\omega \to e^+e^-)$ and $J/\psi \to \phi\pi^+\pi^-\eta'(\phi \to e^+e^-)$, respectively. The nominal masses of η', ω, ϕ are taken from the Particle Data Group [34]. Photons with energy larger than 1.02 MeV may convert to e^+e^- pairs, and this usually occurs in the beam pipe and inner wall of the MDC, leading to a γ conversion background. To reject this background from $J/\psi \to \gamma\pi^+\pi^-\eta'$, the candidate events must satisfy $R_{xy} < 2$ cm, where R_{xy} is the distance from the reconstructed vertex of the e^+e^- pair to the interaction point in the x-y plane based on a γ conversion finder algorithm [38]. With the requirements above, the remaining yields for the $J/\psi \to \gamma X(1835)$, $\gamma X(2120)$, and $\gamma X(2370)$ decays in the MC simulations of the γ conversion background are 32 ± 5, 6 ± 4, 7 ± 8, respectively. These yields are subtracted from the corresponding number of signal events in the fit to data; the same treatment is used for the $\eta' \to \pi^+\pi^-\eta$ decay mode.

For the $\eta' \to \pi^+\pi^-\eta$ decay mode, a five-constraint (5C) kinematic fit imposing conservation of the initial energy and momentum is performed to the $e^+e^-\pi^+\pi^-\pi^+\pi^-\eta$ hypothesis, and the invariant mass of $\gamma\gamma$ candidates is constrained to the known mass of the η meson [34]. For events with more than two photon candidates, the combination with the smallest χ^2_{5C} is selected, and the events with $\chi^2_{5C} < 60$ are retained. The η' candidate is reconstructed

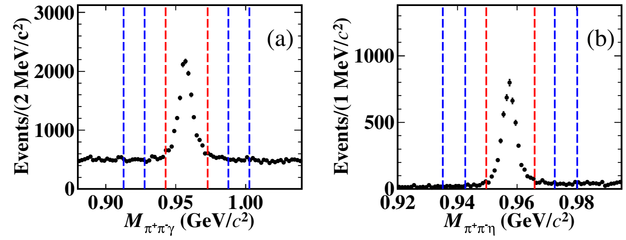

FIG. 1. Invariant-mass distributions for selected (a) $\eta' \to \gamma\pi^+\pi^-$ and (b) $\eta' \to \pi^+\pi^-\eta$ candidates. The dots with error bars are data, the red vertical dashed lines indicate the η' mass windows, and the pairs of blue dashed lines (left and right of the signal peak) indicate the η' sideband regions.

from $\pi^+\pi^-\eta$ combinations in an event, and all combinations are kept. As shown in Fig. 1(b), η' candidates are selected with $|M_{\pi^+\pi^-\eta} - m_{\eta'}| < 8.1\ \mathrm{MeV}/c^2$. The requirements on R_{xy} and $M_{e^+e^-}$ are the same as for the $\eta' \to \gamma\pi^+\pi^-$ decay mode. In total, 20 ± 3, 3 ± 2, and 3 ± 3 events are selected for the $J/\psi \to \gamma X(1835)$, $\gamma X(2120)$, and $\gamma X(2370)$ decay modes in the MC simulations of the γ conversion background.

After imposing the selection criteria described above, a clear $X(1835)$ signal is seen in the invariant-mass spectra of the $\pi^+\pi^-\eta'$ candidates as shown in Fig. 2 for both η' decay modes. Detailed event type analysis of the inclusive MC sample with a generic tool, TOPOANA [39], shows that two classes of potential backgrounds are left after the candidates selection: events with no real η' meson in the final states (non-η'), and events from $J/\psi \to \pi^0\pi^+\pi^-\eta'$ decays.

In Ref. [3], two models were used to characterize the $\pi^+\pi^-\eta'$ line shape around $1.85\ \mathrm{GeV}/c^2$: one incorporates the opening of a threshold in the mass spectrum (Flatté formula), and the other is the coherent sum of two resonant amplitudes. Since our fit range reaches up to $2.8\ \mathrm{GeV}/c^2$, the long and high tail of the Flatté formula in the higher range of the first model makes the fit unstable. We therefore consider the other model, which assumes the existence of a narrow resonance $X(1870)$ near the $p\bar{p}$ threshold, with the interference between this resonance and the $X(1835)$ causing the line-shape distortion. Thus, the anomalous line shape near $1.835\ \mathrm{GeV}/c^2$ rate is modeled as $|T|^2$, where T is the decay amplitude of a coherent sum of the two Breit-Wigner functions for $X(1835)$ and $X(1870)$, defined in Eq. (3) of Ref. [3]. It is known from Ref. [40] that there should be two nontrivial solutions in a fit using a coherent sum of two Breit-Wigner functions. So Ref. [3] obtained two solutions with constructive and destructive interference in their fit to the $M_{\pi^+\pi^-\eta'}$ spectra. The two solutions share the same mass and width of the $X(1835)$ and $X(1870)$, but have different values of the relative $\pi^+\pi^-\eta'$ coupling strengths and the phase between the two resonances, which means that the only observable difference between the solutions are branching fractions of the

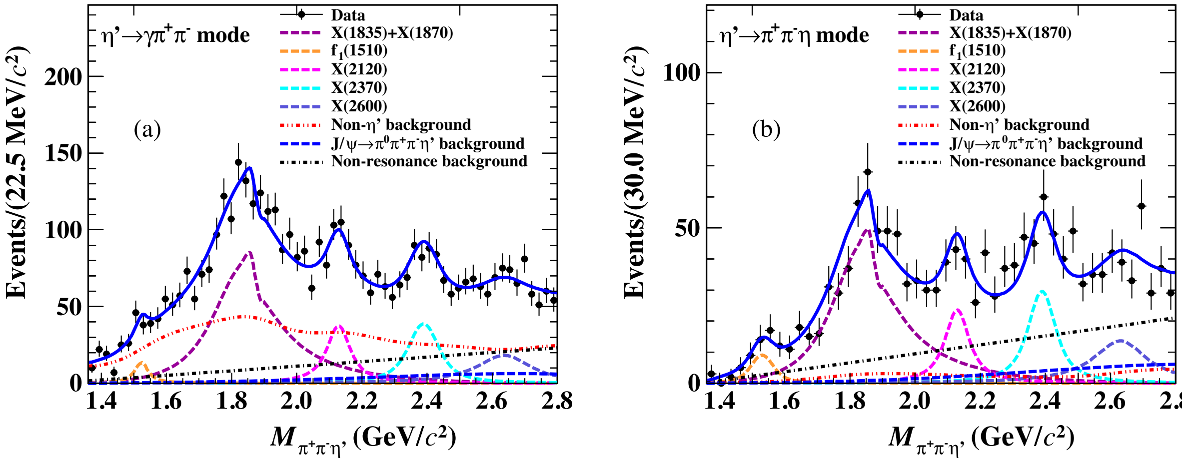

FIG. 2. Invariant-mass distributions $M_{\pi^+\pi^-\eta'}$ for selected $\eta' \to \gamma\pi^+\pi^-$ candidates for the (a) $\eta' \to \gamma\pi^+\pi^-$ decay mode and (b) $\eta' \to \pi^+\pi^-\eta$ decay mode. A simultaneous unbinned maximum likelihood fit on the spectra determines the signal yields of the intermediate resonances from both of the η' decay modes simultaneously. The dots with error bars are data, the blue solid line is the total fit, the orange dashed line describes the $f_1(1510)$ resonance, the purple dashed line—the $X(1835)$ and $X(1870)$ states, the pink dashed line—the $X(2120)$ state, the cyan dashed line—the $X(2370)$ state, the light blue dashed line—the $X(2600)$ state, the red dashed line indicates the non-η' background, the blue dashed line is the $J/\psi \to \pi^0\pi^+\pi^-\eta'$ background, and the black dot-dashed line corresponds to a Chebyshev polynomial function describing possible nonresonance backgrounds.

two Breit-Wigner functions. All of the above parameters of T in our fit are fixed to the measured values in Ref. [3] and consequently there will be two sets of branching fractions for $J/\psi \to e^+e^-X(1835)$, $X(1835) \to \pi^+\pi^-\eta'$ decay as shown in Table I.

The $M_{\pi^+\pi^-\eta'}$ spectra for the two η' decay modes in the range from 1.36 to 2.80 GeV/c^2 are shown in Fig. 2. A simultaneous unbinned maximum likelihood fit on the spectra determines the signal yields of the intermediate resonances from both of the η' decay modes simultaneously. Because of low statistics and unknown variations across the X Dalitz plot, the only interference considered is that within the amplitude T. The effect of the six intermediate resonances are described by the sum of five terms. The first contains two resonances,

$$(|T|^2 \times \epsilon_{\mathrm{sig}}) \otimes g, \tag{2}$$

and the remaining four terms are of the form

$$(|BW|^2 \times \epsilon_{\mathrm{sig}}) \otimes g. \tag{3}$$

TABLE I. Branching fractions of $J/\psi \to e^+e^-X$, $X \to \pi^+\pi^-\eta'$ decays. The first uncertainties are statistical, and the second are systematic.

Branching fractions of $J/\psi \to e^+e^-X$, $X \to \pi^+\pi^-\eta'$		
$X = X(1835)$	(solution I)	$(3.58 \pm 0.19 \pm 0.16) \times 10^{-6}$
	(solution II)	$(4.43 \pm 0.23 \pm 0.19) \times 10^{-6}$
$X = X(2120)$		$(0.82 \pm 0.12 \pm 0.06) \times 10^{-6}$
$X = X(2370)$		$(1.08 \pm 0.14 \pm 0.10) \times 10^{-6}$

Here, ϵ_{sig} is the mass-dependent detection efficiency; g is a Gaussian function used to account for the mass resolution. The motivation for the T in Eq. (2) was discussed above. The other resonances, i.e., $f_1(1510)$, $X(2120)$, $X(2370)$, and $X(2600)$ are described by Eq. (3) in the fit, where $|BW|^2$ is the Breit-Wigner function for $f_1(1510)$, $X(2120)$, $X(2370)$, and $X(2600)$. The masses and widths of the first three resonances are fixed to the values in Ref. [2,15]. Possible background contribution from non-η' background processes is estimated by the events in the η' mass sideband. To estimate the contribution from the $J/\psi \to \pi^0\pi^+\pi^-\eta'$ process, a phase space MC-simulation sample is generated and parametrized by a fourth-order Chebyshev polynomial function. In addition to these two background processes, a first-order Chebyshev polynomial function is used to describe possible nonresonance background processes. The fit yields are 77 ± 23, 1364 ± 53, 310 ± 32, 397 ± 37, and 323 ± 62 events for $f_1(1510)$, $X(1835)$ with $X(1870)$, $X(2120)$, $X(2370)$, and $X(2600)$, respectively. The statistical significance is determined from the change of the log likelihoods with and without the corresponding signal shape. The effect of the assumed background and signal shapes are also considered when evaluating the significance. Variations are tested, and the lowest significances of the $f_1(1510)$, $X(1835)$, $X(2120)$, $X(2370)$, and $X(2600)$ states are calculated to be 3.3σ, 15σ, 5.3σ, 7.3σ, and 3.2σ, respectively.

The TFF $|F(q^2)|^2$ for the process $J/\psi \to e^+e^-X(1835)$ is measured by dividing the $M_{e^+e^-}$ distribution into five intervals. The values of $|F(q^2)|^2$ are obtained as the ratios of branching fractions measured with the fit method described above and those predicted by QED in each

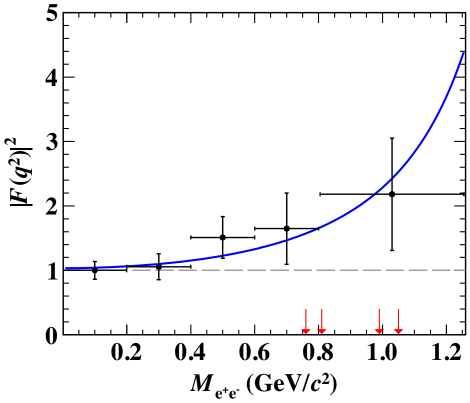

FIG. 3. $|F(q^2)|^2$ distribution for $J/\psi \to e^+e^-X(1835)$ decays. The dots with error bars are $|F(q^2)|^2$ values, the solid blue curve is the fit result according to the simple pole approximation, and the gray dashed line represents $|F(q^2)|^2 = 1$. The red arrows denote the $M_{e^+e^-}$ veto requirements.

interval as shown in Eq. (1). These QED predicted branching fractions are obtained from Eq. (12) of Ref. [18]. Figure 3 shows the values of $|F(q^2)|^2$ determined in each interval of the $M_{e^+e^-}$ distribution. A simple pole approximation parametrized as $F(q^2) = [1/(1 - q^2/\Lambda^2)]$ [18,19], where the parameter Λ is the spectroscopic pole mass, is used to fit the distribution. From the fit, Λ is determined to be $[1.75 \pm 0.29(\mathrm{stat}) \pm 0.05(\mathrm{syst})]$ GeV/c^2. The systematic uncertainty is taken as the difference between the baseline Λ value and the refitted one including the systematic uncertainties of the measured branching fractions in each interval.

The systematic uncertainties on the branching fractions associated with the efficiency include the signal generator, photon detection efficiency, tracking efficiency, particle identification efficiency, kinematic fit, mass spectra requirements [γe^+e^-, $\pi^+\pi^-$, $\pi^+\pi^-\gamma(\eta)$, and e^+e^-], and R_{xy} requirement. The uncertainties from these efficiency-related sources are 3.7%, 4.9%, and 7.2% for the $X(1835)$, $X(2120)$, and $X(2370)$ modes, respectively. The total systematic uncertainties related to fit methods include the non-η' background, $J/\psi \to \pi^0\pi^+\pi^-\eta'$ background, nonresonance background, and signal shape. The total uncertainties due to the fit are 1.3%, 4.5%, and 4.7% for the $X(1835)$, $X(2120)$, and $X(2370)$ modes, respectively. Additional uncertainties for the total number of J/ψ events [28] and the η' branching fractions to the final states $\gamma\pi^+\pi^-$ and $\pi^+\pi^-\eta$ [34] are also included. The total for all systematic uncertainties on the product branching fractions of the $X(1835)$, $X(2120)$, and $X(2370)$ modes are 4.3%, 6.8%, and 8.8%, respectively. The final branching fraction results are shown in Table I.

In summary, using a sample of about 10^{10} J/ψ events collected at the center-of mass energy $\sqrt{s} = 3.097$ GeV with the BESIII detector, we report the observation of the EM Dalitz decay $J/\psi \to e^+e^-\pi^+\pi^-\eta'$. This is also the first observation of the states $X(1835)$, $X(2120)$, and $X(2370)$ in the EM Dalitz decays, and the first measurement of the TFF between J/ψ and $X(1835)$. According to the model of a coherent sum of two Breit-Wigner amplitudes of $X(1835)$ and $X(1870)$, the branching fraction of $J/\psi \to e^+e^-X(1835)$, $X(1835) \to \pi^+\pi^-\eta'$ is measured to be $[3.58 \pm 0.19(\mathrm{stat}) \pm 0.16(\mathrm{syst})] \times 10^{-6}$ (constructive interference)/$[4.43 \pm 0.23(\mathrm{stat}) \pm 0.19(\mathrm{syst})] \times 10^{-6}$ (destructive interference) with a significance of 15σ. With respect to the radiative decay $J/\psi \to \gamma X(1835)$, $X(1835) \to \pi^+\pi^-\eta'$ [3], the ratio R of the branching fractions is determined to be $[1.19 \pm 0.10(\mathrm{stat}) \pm 0.14(\mathrm{syst})] \times 10^{-2}$. The measured R is consistent with the theoretical prediction [17] within 2 standard deviations (2σ). The branching fractions of $J/\psi \to e^+e^-X(2120)$, $X(2120) \to \pi^+\pi^-\eta'$ and $J/\psi \to e^+e^-X(2370)$, $X(2370) \to \pi^+\pi^-\eta'$ are measured to be $[0.82 \pm 0.12(\mathrm{stat}) \pm 0.06(\mathrm{syst})] \times 10^{-6}$ and $[1.08 \pm 0.14(\mathrm{stat}) \pm 0.10(\mathrm{syst})] \times 10^{-6}$ with significances of 5.3σ and 7.3σ, respectively. The measured values of $|F(q^2)|^2$ for the $J/\psi \to e^+e^-X(1835)$ channel deviate from the pointlike particle assumption ($|F(q^2)|^2 = 1$) significantly and have been parametrized in the simple pole approximation as $F(q^2) = [1/(1 - q^2/\Lambda^2)]$ with $\Lambda = [1.75 \pm 0.29(\mathrm{stat}) \pm 0.05(\mathrm{syst})]$ GeV/c^2. This measured pole mass Λ can be used as an input parameter to improve the theoretical calculations.

The BESIII collaboration thanks the staff of BEPCII and the IHEP computing center for their strong support. The authors thank Xian-Wei Kang for useful discussions. This work is supported in part by National Key R&D Program of China under Contracts No. 2020YFA0406300, No. 2020YFA0406400; National Natural Science Foundation of China (NSFC) under Contracts No. 11805037, No. 11625523, No. 11635010, No. 11735014, No. 11822506, No. 11835012, No. 11935015, No. 11935016, No. 11935018, No. 11961141012, No. 12022510, No. 12025502, No. 12035009, No. 12035013, No. 12061131003; the Chinese Academy of Sciences (CAS) Large-Scale Scientific Facility Program; Joint Large-Scale Scientific Facility Funds of the NSFC and CAS under Contracts No. U1832121, No. U1632107, No. U1732263, No. U1832207; CAS Key Research Program of Frontier Sciences under Contract No. QYZDJ-SSW-SLH040; 100 Talents Program of CAS; INPAC and Shanghai Key Laboratory for Particle Physics and Cosmology; ERC under Contract No. 758462; European Union Horizon 2020 research and innovation programme under Marie Sklodowska-Curie grant agreement under Contract No. 894790; German Research Foundation DFG under Contract No. 443159800, Collaborative Research Center CRC 1044, FOR 2359, GRK 214; Istituto Nazionale di Fisica Nucleare, Italy; Ministry of Development of Turkey under Contract No. DPT2006K-120470; National Science and Technology fund; Olle Engkvist Foundation under Contract No. 200-0605; STFC (United Kingdom); The Knut and Alice Wallenberg Foundation (Sweden) under Contract No. 2016.0157; The Royal Society, UK under Contracts No. DH140054, No. DH160214; The Swedish Research Council; U.S. Department of Energy under Contracts No. DE-FG02-05ER41374, No. DE-SC-0012069.

[a]Also at Bogazici University, 34342 Istanbul, Turkey.
[b]Also at the Moscow Institute of Physics and Technology, Moscow 141700, Russia.
[c]Also at the Novosibirsk State University, Novosibirsk 630090, Russia.
[d]Also at the NRC "Kurchatov Institute", PNPI, 188300 Gatchina, Russia.
[e]Also at Istanbul Arel University, 34295 Istanbul, Turkey.
[f]Also at Goethe University Frankfurt, 60323 Frankfurt am Main, Germany.
[g]Also at Key Laboratory for Particle Physics, Astrophysics and Cosmology, Ministry of Education; Shanghai Key Laboratory for Particle Physics and Cosmology; Institute of Nuclear and Particle Physics, Shanghai 200240, People's Republic of China.
[h]Also at Key Laboratory of Nuclear Physics and Ion-beam Application (MOE) and Institute of Modern Physics, Fudan University, Shanghai 200443, People's Republic of China.
[i]Also at Harvard University, Department of Physics, Cambridge, Massachusetts 02138, USA.
[j]Present address: Institute of Physics and Technology, Peace Avenue 54B, Ulaanbaatar 13330, Mongolia.
[k]Also at State Key Laboratory of Nuclear Physics and Technology, Peking University, Beijing 100871, People's Republic of China.
[l]Also at School of Physics and Electronics, Hunan University, Changsha 410082, China.
[m]Also at Guangdong Provincial Key Laboratory of Nuclear Science, Institute of Quantum Matter, South China Normal University, Guangzhou 510006, China.
[n]Also at Frontier Science Center for Rare Isotopes, Lanzhou University, Lanzhou 730000, People's Republic of China.
[o]Also at Lanzhou Center for Theoretical Physics, Lanzhou University, Lanzhou 730000, People's Republic of China.

[1] M. Ablikim *et al.* (BES Collaboration), Phys. Rev. Lett. **95**, 262001 (2005).
[2] M. Ablikim *et al.* (BESIII Collaboration), Phys. Rev. Lett. **106**, 072002 (2011).
[3] M. Ablikim *et al.* (BESIII Collaboration), Phys. Rev. Lett. **117**, 042002 (2016).
[4] M. Ablikim *et al.* (BESIII Collaboration), Phys. Rev. Lett. **115**, 091803 (2015).
[5] M. Ablikim *et al.* (BESIII Collaboration), Phys. Rev. D **97**, 051101(R) (2018).
[6] J. Z. Bai *et al.* (BES Collaboration), Phys. Rev. Lett. **91**, 022001 (2003).
[7] M. Ablikim *et al.* (BESIII Collaboration), Phys. Rev. Lett. **108**, 112003 (2012).
[8] J. P. Alexander *et al.* (CLEO Collaboration), Phys. Rev. D **82**, 092002 (2010).
[9] B. S. Zou and H. C. Chiang, Phys. Rev. D **69**, 034004 (2004).
[10] X. Liu, X. Q. Zeng, and Y. B. Ding *et al.*, arXiv:hep-ph/0406118.
[11] A. Datta and P. J. O'Donnell, Phys. Lett. B **567**, 273 (2003).
[12] S. B. Athar *et al.* (CLEO Collaboration), Phys. Rev. D **73**, 032001 (2006).
[13] M. Ablikim *et al.* (BESIII Collaboration), Phys. Rev. D **87**, 112004 (2013).
[14] M. Ablikim *et al.* (BESIII Collaboration), Phys. Rev. D **93**, 052010 (2016).
[15] M. Ablikim *et al.* (BESIII Collaboration), arXiv:2201.10796.
[16] L. G. Landsberg, Phys. Rep. **128**, 301 (1985).
[17] J. L. Zhang, J. J. He, T. J. Zhu, S. Q. Xu, and R. M. Wang, Int. J. Mod. Phys. A **34**, 1950129 (2019).
[18] L. M. Gu, H. B. Li, X. X. Ma, and M. Z. Yang, Phys. Rev. D **100**, 016018 (2019).
[19] J. L. Fu, H. B. Li, X. S. Qin, and M. Z. Yang, Mod. Phys. Lett. A **27**, 1250223 (2012).
[20] N. M. Kroll and W. Wada, Phys. Rev. **98**, 1355 (1955).
[21] B. A. Li, Phys. Rev. D **74**, 034019 (2006).
[22] G. Hao, C. F. Qiao, and A. L. Zhang, Phys. Lett. B **642**, 53 (2006).
[23] X. G. He, X. Q. Li, X. Liu, and J.-P. Ma, Eur. Phys. J. C **49**, 731 (2007).
[24] T. Huang and S. L. Zhu, Phys. Rev. D **73**, 014023 (2006).
[25] C. Q. Pang, Phys. Rev. D **99**, 074015 (2019).
[26] H. Y. Cheng and X. W. Kang, Phys. Lett. B **780**, 100 (2018).
[27] C. H. Yu *et al.*, *Proceedings of the 7th International Particle Accelerator Conference (IPAC'16), Busan, Korea, 2016*, (JACoW Publishing, Geneva, Switzerland, 2016), pp. 1014–1018, 10.18429/JACoW-IPAC2016-TUYA01.
[28] M. Ablikim *et al.* (BESIII Collaboration), arXiv:2111.07571 [Chin. Phys. C (to be published)].
[29] M. Ablikim *et al.* (BESIII Collaboration), Nucl. Instrum. Methods Phys. Res., Sect. A **614**, 345 (2010).
[30] M. Ablikim *et al.* (BESIII Collaboration), Chin. Phys. C **44**, 040001 (2020).
[31] S. Agostinelli *et al.* (GEANT4 Collaboration), Nucl. Instrum. Methods Phys. Res., Sect. A **506**, 250 (2003).
[32] S. Jadach, B. F. L. Ward, and Z. Was, Phys. Rev. D **63**, 113009 (2001); Comput. Phys. Commun. **130**, 260 (2000).
[33] D. J. Lange, Nucl. Instrum. Methods Phys. Res., Sect. A **462**, 152 (2001); R. G. Ping, Chin. Phys. C **32**, 599 (2008).
[34] P. A. Zyla *et al.* (Particle Data Group), Prog. Theor. Exp. Phys. **2020**, 083C01 (2020).
[35] J. C. Chen, G. S. Huang, X. R. Qi, D. H. Zhang, and Y. S. Zhu, Phys. Rev. D **62**, 034003 (2000).
[36] R. L. Yang, R. G. Ping, and H. Chen, Chin. Phys. Lett. **31**, 061301 (2014).
[37] E. Richter-Was, Phys. Lett. B **303**, 163 (1993).
[38] Z. R. Xu and K. L. He, Chin. Phys. C **36**, 742 (2012).
[39] X. Y. Zhou, S. X. Du, G. Li, and C. P. Shen, Comput. Phys. Commun. **258**, 107540 (2021).
[40] K. Zhu, X. H. Mo, C. Z. Yuan, and P. Wang, Int. J. Mod. Phys. A **26**, 4511 (2011).